

Modeling the Earliest Stages of Gliomagenesis Using Human iPSC-derived NPCs in A Three-dimensional Alginate-based Matrix

Üç Boyutlu Aljinat-bazlı Bir Matriste İnsan iPSC'lerinden Türetilmiş NPC'leri Kullanarak Gliomagenезin En Erken Aşamalarının Modellenmesi

© Burcu Ekinci¹, © Tutku Yaraş², © Yavuz Oktay³

¹Dokuz Eylül University, Izmir International Biomedicine and Genome Institute, Izmir, Turkey

²Izmir Biomedicine and Genome Center, Izmir, Turkey

³Dokuz Eylül University, Faculty of Medicine, Department of Medical Biology, Izmir, Turkey

Cite as: Ekinci B, Yaraş T, Oktay T. Modeling the Earliest Stages of Gliomagenesis Using Human iPSC-derived NPCs in A Three-dimensional Alginate-based Matrix. Anatol J Gen Med Res 2023;33(3):362-73

Abstract

Objective: The development of gliomas is believed to be triggered by isocitrate dehydrogenase (IDH1/2) mutations, but there is limited information on how IDH1/2 mutations trigger gliogenesis. This is because studies over the years have often used patient tumor samples, transformed cells, or normal stem cells with driver mutations to explore the early stages of glioma development. In this study, we constructed a model to understand the specific effects of IDH1-R132H mutation alone by preparing an alginate-based 3D culture with NPCs and hence sought to avoid the effects of other driver mutations.

Methods: Human induced pluripotent stem cells were differentiated into neural progenitor cells (NPCs). NPCs embedded in an alginate-based 3D matrix were incubated in neural progenitor medium for 1 day (day 0). Neural Progenitor Medium was then removed from the NPC-alginate beads and incubated for 14 days with conditioned media from immortalized human astrocytes (IHAs) that produced doxycycline-induced wild-type IDH1 and mutant IDH1. On day 14, IHA-conditioned media were replaced with Neural Progenitor Medium and incubated for 3 days (day 17). RNA was isolated from NPCs on days 0 and 17, and key genes [Tet methylcytosine dioxygenase 1 (TET1) and Mesenchyme Homeobox 2 (MEOX2)] previously reported to be altered in IDH1-mutant gliomas, were evaluated by RT-qPCR.

Results: Optimal alginate-based 3D culture conditions were established using NPCs. Expression of key genes was examined on days 0 and 17. In the NPC-alginate bead 3D culture model, TET1 was upregulated and MEOX2 tended to be downregulated after exposure to IHA-IDH1-R132H conditioned medium.

Conclusion: We have developed a novel NPC-alginate bead 3D culture model for the first time in the literature. By recapitulating the earliest stages of gliomagenesis, this model will allow the study of the effects of the IDH1-R132H mutation without confounding the effects of the other mutations.

Keywords: Glioma, isocitrate dehydrogenase, IDH1, immortalized human astrocytes, neural progenitor cells, NPCs

Öz

Amaç: Glioma gelişiminin izositrat dehidrojenaz (IDH1/2) mutasyonları tarafından tetiklendiğine inanılmaktadır, ancak IDH1/2 mutasyonlarının gliomagenезi nasıl tetiklediğine dair sınırlı bilgi bulunmaktadır. Bunun nedeni, yıllar boyunca yapılan çalışmalarda, glioma gelişiminin erken aşamalarını araştırmak için sıklıkla hasta tümör örneklerini veya dönüştürülmüş hücreleri veya sürücü mutasyonlara sahip normal kök hücreleri kullanmasıdır. Burada, NPC'lerle aljinat



Address for Correspondence/Yazışma Adresi: Burcu Ekinci, Dokuz Eylül University, Izmir International Biomedicine and Genome Institute, Izmir, Turkey
Phone: +90 506 537 35 62 **E-mail:** b.burcuekinci@gmail.com
ORCID ID: orcid.org/0000-0001-5408-7584

Received/Geliş tarihi: 26.08.2023
Accepted/Kabul tarihi: 30.10.2023



Copyright© 2023 The Author. Published by Galenos Publishing House on behalf of University of Health Sciences Turkey, Izmir Tepecik Training and Research Hospital. This is an open access article under the Creative Commons AttributionNonCommercial 4.0 International (CC BY-NC 4.0) License.

Öz

bazlı bir 3 boyutlu kültür hazırlayarak tek başına IDH1-R132H mutasyonunun spesifik etkilerini anlamak için bir model oluşturduk ve dolayısıyla diğer sürücü mutasyonlarının etkilerinden kaçınmaya çalıştık.

Yöntem: İnsan İndüklenmiş Pluripotent Kök Hücreler (hiPSC'ler), Nöral Progenitör Hücrelere (NPC'ler) farklılaştırıldı. Aljinat bazlı bir 3D matrise gömülü NPC'ler, Nöral Progenitör Ortamında 1 gün (0. gün) boyunca inkübe edildi. Daha sonra, Nöral Progenitör Ortamı, NPC-aljinat boncuklarından uzaklaştırıldı ve doksisisiklin kaynaklı vahşi tip IDH1 ve Mutant IDH1 üreten Ölümsüzleştirilmiş İnsan Astrositlerinden (IHA'lar) şartlandırılmış ortamlarla 14 gün boyunca inkübe edildi. On dördüncü günde, IHA koşullu ortam, Nöral Progenitör Ortamı ile değiştirildi ve 3 gün boyunca (17. gün) inkübe edildi. RNA, 0. ve 17. günde NPC'lerden izole edildi ve daha önce IDH1 mutant gliomalarda değiştirildiği bildirilen anahtar genler [Tet metilsitozin dioksijenaz 1 (TET1) ve Mesenchyme Homeobox 2 (MEOX2)] RT-qPCR ile değerlendirildi.

Bulgular: NPC'lerle optimum aljinat bazlı 3 boyutlu kültür koşulları oluşturuldu. Anahtar genlerin ekspresyonu 0. günde ve 17. günde incelendi. NPC-aljinat boncuk 3D kültür modelinde, TET1 yukarı regüle edildi ve MEOX2, IHA-IDH1-R132H koşullu ortama maruz bırakıldıktan sonra aşağı regüle edilme eğilimindeydi.

Sonuç: Literatürde ilk kez yeni bir NPC-aljinat boncuk 3 boyutlu kültür modeli geliştirdik. Bu model, gliomajenezin en erken aşamalarını taklit ederek, diğer mutasyonların karıştırıcı etkileri olmadan IDH1-R132H mutasyonunun etkilerini inceleme olanağı sağlayacaktır.

Anahtar Kelimeler: Glioma, izositrat dehidrojenaz, IDH1, ölümsüzleştirilmiş insan astrositleri, nöral progenitör hücreler, NPC'ler

Introduction

Gliomas, a deadly brain tumor type, have poor prognosis, high morbidity and mortality, and are rare compared with other tumors⁽¹⁾. According to data from the Central Brain Tumor Registry of the United States, the worldwide incidence rate of primary malignant brain and other CNS tumors was 3.5 per 100,000 population⁽²⁾.

Gliomas, the most common type of cancer arising from brain tissue, are devastating cancers that are often incurable because of their heterogeneity and invasive properties^(3,4). Current treatment modalities such as surgical resection, radiation, and chemotherapy provide modest benefits for patient survival^(5,6), and no significant advances have been made in the treatment of gliomas in the past >20 years^(6,7).

Isocitrate dehydrogenases (IDH), whose mutations are one of the most important diagnostic markers of gliomas, act as core metabolic enzymes in the citric acid cycle and convert isocitrate to α -ketoglutarate (α -KG)^(8,9). Mutations in IDH1 or IDH2 enzymes in lower-grade glioma (LGG) and secondary GBMs are usually heterozygous missense mutations and frequently affect amino acids 132 of IDH1 and 172 of IDH2⁽¹⁰⁾.

Mutated IDH1 and IDH2 enzymes acquire a neomorphic feature, leading to the production of 2-hydroxyglutarate, an oncometabolite⁽⁶⁾. 2-HG is structurally similar to α -KG and competitively inhibits α -KG-dependent dioxygenases, including DNA demethylases (e.g., TET family) and histone demethylases (e.g., Jumonji family)^(11,12). As a result, the epigenetic landscape of histones and DNA changes, which

results in numerous cellular changes⁽¹³⁻¹⁵⁾. *IDH1/2* mutations are considered to be the earliest genetic alterations that trigger the development of gliomas, as they have been shown to precede mutations in genes, such as *TP53* mutations known to play roles in glioma development, the glioma-specific 1p/19q codeletion, or the genome-wide CpG island methylator phenotype (G-CIMP)⁽¹⁶⁾.

Existing cellular models to mimic early gliogenesis often include transformed cells or normal stem cells with driver mutations, such as those in *TP53*, *ATRX*, 1p/19q codeletion, *EGFR*, *PTEN*, *NF1*, *CDKN2A/B*, et. Although the origins of gliomas remain unclear, studies in developmental biology, patients, and experimental glioma models suggest that glioma origins may be neural progenitor or stem cells, oligodendrocyte precursor/progenitor cells, or astrocytes⁽¹⁷⁾.

Self-renewing, multipotent, and GFAP-expressing neural stem cells (NSCs) transform into neural progenitor cells (NPCs) that generate neurons and glial cells^(18,19). Because of the developmental potential and plasticity of NSCs, they are ideal candidates for glioma cells of origin because multiple oncogenic mutations are required for gliomagenesis, and the self-renewal and proliferative properties of NSCs may result in the endogenous accumulation of somatic mutations^(20,21). However, the role of postmitotic and differentiated astrocytes in glioma formation is still debated⁽²⁰⁾.

Previous studies have often used 2D cultures that force cells to adapt to an artificial, flat, and hard surface. 2D cultures can alter the metabolism and degree of functionality of cells, which may significantly differ from the behavior of cells *in vivo*^(22,23).

In contrast, 3D cellular systems reflect and allow the study of biological processes such as interactions between cells, the effect of the extracellular matrix on cells, and different external physical and chemical stimuli⁽²⁴⁻²⁶⁾. Alginate derived from algae is the most widely used natural polymer for microencapsulation because of its permeability, biocompatibility, long-term stability, and water retention ability. Unmodified alginate is ionically crosslinked by activation with divalent cations such as Ca^{2+} ⁽²⁷⁾. Alginate is used during differentiation of stem cells into neural lineages because it successfully mimics the 3D environment of the central nervous system^(28,29). Therefore, we decided to use alginate to develop a novel model of the earliest stages of gliogenesis.

Our knowledge of how the cascade initiated by *IDH1/2* mutations triggers or facilitates gliogenesis is limited. In comprehensive multi-omic studies that have been ongoing for years, either patient tumor samples or glioma models created by combining many oncogenic mutations were used. However, *IDH1/2* mutations are known to be genetic changes that occur at the earliest stage of gliomagenesis; therefore, models with additional mutations may not recapitulate the oncogenic changes leading to glioma development. In this study, we have shown that the NPC-alginate bead 3D culture model combined with conditioned media from immortalized human astrocytes (IHAs) expressing mutant *IDH1* inducibly is a suitable model to examine the earliest stages of gliomagenesis and how the *IDH1-R132H* mutation affects cells with brain tumor initiation potential. Importantly, this model is the first to reveal how the *IDH1-R132H* mutation alone acts in the earliest stages of gliomagenesis, independent of the confounding oncogenic effects of other driver mutations that are used in the existing models generated to date.

Materials and Methods

Immortalized Human Astrocytes

IHAs were a gift from Prof. Timothy Chan, assisted by Dr. Sevin Turcan. IHA-*IDH1*-WT and IHA-*IDH1-R132H* cells were induced by doxycycline (Sigma, Cat No: D9891-5G) to produce wild-type (WT) *IDH1* and mutant *IDH1*, respectively. IHA cells were maintained in DMEM High glucose (Gibco, Cat No: 41965-039) supplemented with 10% FBS (Gibco, Cat No: 10500-064) and penicillin/streptomycin (Gibco, Cat No: 15140122).

To produce IHA-*IDH1*-WT and IHA-*IDH1-R132H* conditioned media, IHA-*IDH1*-WT and IHA-*IDH1-R132H* cells were

cultured in DMEM high glucose medium in the presence of doxycycline. When the cells reached 80-90% confluency, media in which the cells were cultured were collected, filtered with 0.45 M filter, and stored at -20 °C. After IHA-*IDH1*-WT and IHA-*IDH1-R132H* conditioned media were removed, IHA-*IDH1*-WT and IHA-*IDH1-R132H* cells were passaged with trypsin and grown in 1 µg/mL doxycycline-containing DMEM High Glucose.

hiPS Cell Culture

Mouse embryonic fibroblast (MEF) cells were cultured in MEF medium (DMEM High Glucose, 10% FBS, 2mM GlutaMAX, 1% pen/strep, 1X MEM-NEAA and 1X Sodium Pyruvate) in a gelatin-coated 6-well plate. When the confluency of MEF cells in a plate reached 85-90%, cells were treated with mitomycin C (Biovision, Cat No: 2713-5) at a final concentration of 10 µg/mL for 3 h at 37 °C and 5% CO_2 .

After incubation, medium containing mitomycin C was aspirated and cells were washed with DMEM High Glucose. Human iPSCs were opened with HESC medium (DMEM-F12 medium, 20% Knock-out SR, 1X MEM-NEAA, 2-Mercaptoethanol, 15mM HEPES and 100 ng/mL bFGF) on mitotically inactivated MEF feeder cells. Cells were incubated at 37 °C and 5% CO_2 , and the medium was changed every day with fresh HESC medium. When iPSC colonies reached sufficient size, they were detached with dispase in DMEM-F12 (Stemcell Technologies, Cat No: 07923). The hiPSC colonies were cultured in mTESR™ 1 complete medium (mTESR Basal Medium and mTESR 5X Supplement) in matrigel (Corning, Cat No: 354277) coated wells of a 6-well plate. When cells reached 70%–80% confluency, colonies were removed with dispase and replated in fresh mTESR™ 1 complete medium in a 6-well plate.

Generating NPCs from human iPS cells

To NPCs from hiPSCs, "Generation and Culture of NPCs using the STEMdiff™ Neural System" monolayer culture protocol from STEMCELL Technologies was used. First, after iPSC colonies were washed with sterile PBS, the cells were dissociated with Gentle Cell Dissociation Reagent (StemCell, Cat No: 07174). Cells in STEMdiff™ Neural Induction Medium + SMADi (StemCell, Cat No: 08581) were plated in a single well of a matrigel-coated 6-well plate and incubated at 37 °C and 5% CO_2 . Every day, the whole medium was replaced with fresh STEMdiff™ Neural Induction Medium + SMADi until cell confluency reached 90%. Cells were treated with accutane (Stemcell, Cat No: 07923) and then cells in STEMdiff™

Neural Induction Medium + SMADi were cultured in a well of a Matrigel- coated 6-well plate. Cells were passaged once more and plated with STEMdiff™ Neural Induction Medium + SMADi. After two passages, the neural progenitor cell culture protocol was used for the expansion of NPCs.

Cells were treated with accutane and plated in a matrigel-coated 6-well plate in STEMdiff™ Neural Progenitor Medium (Stemcell, Cat No: 05833). At 90% confluency, cells were passaged and placed in fresh STEMdiff™ Neural Progenitor Medium in a matrigel-coated 6-well plate. Ethical approval for the study was obtained from İzmir Biomedicine and Genome Center

Non-Invasive Research Ethics Committee (ethical approval number: 2020-042).

Immunofluorescence staining for the characterization of hiPSCs and NPCs

Cells were seeded on Matrigel- coated coverslips in 24-well plates. After cells were attached to the coverslips and were 50-60% confluent, they were fixed with 4% paraformaldehyde (Sigma-Aldrich, Cat No: 158127-100G) for 15 min at RT. Then, cells attached to coverslips were washed with 1X PBS three times. They were permeabilized with 0.1% Triton X-100 in 1X PBS for 10 min at RT. After 10 min, cells were washed with 1X PBS three times. For blocking, 1% BSA in PBST (PBS with 0.1% Tween-20) was added to the cells and incubated for 1 h at RT. Cells were incubated with primary antibodies in blocking solution for 2 h at room temperature. NPCs were detected with mouse NESTIN (1:1500, Cell Signaling, Cat No: 33475), rabbit SOX2 (1:400, Cell Signaling, Cat No: 3579), rabbit SOX1 (1:400, Cell Signaling, Cat No: 4194S), mouse OCT4 (1:200, Cell Signaling, Cat No: 75463), and rabbit PAX6 (1:200, Cell Signaling, Cat no: 60433). iPSCs were detected using Mouse OCT4 (1:200, Cell Signaling, Cat No: 75463). After primary antibody staining, cells were washed with 1X PBS three times. Secondary antibodies in blocking solution were added to cells and incubated for 1 h at RT in the dark. Goat anti-rabbit conjugated to Alexa 555 (1:500, Abcam, Cat No: ab150078) and goat anti-mouse conjugated to Alexa 488 (1:500, Abcam, Cat No: ab150113) were applied. After washing with 1 PBS three times, cells were counterstained with Hoechst (1:1000) in PBS to stain nuclei for 3 min at RT. The cells were then washed with 1 PBS. Cover slips were flipped onto a drop of mounting medium placed on a slide.

Alginate-Based 3D NPC Culture

Alginate solution (2%) (Sigma, Cat No: 1112) was prepared with ddH₂O and autoclaved. This solution was filtered with a 0.2 µM filter and then stored +4 °C. When alginate beads formed with NPCs were prepared, neural progenitor medium and 2% alginate solution were mixed equally. The concentration of alginate solution was reduced from 2% to 1% with the medium.

Before embedding NPCs in alginate beads, accutane was used to collect NPCs from 10-cm plates. Viable cells were counted using Trypan Blue and a hemocytometer. Each alginate bead consists of 10 µL of alginate solution formed using a syringe with a 21G 1-12" needle. Cells were centrifuged, supernatants were removed, and the volume of 1% alginate solution to be added was adjusted so that the cell concentration in alginate was 250,000 cells/mL. Cell- alginate suspension was dropped onto 100 mM CaCl₂ buffer with the help of a syringe to form alginate beads containing NPCs. The CaCl₂ buffer was removed and the cells were washed with DMEM-F12. After the washing step, neural progenitor medium was added to NPC-alginate beads and incubated at 37 °C and 5% CO₂.

Three different time points (Day 0, Day 14 and Day 17) and 5 different experimental conditions were selected to develop the model.

In the first group (control), there was no manipulation of cells. NPC-alginate beads were incubated in neural progenitor medium for 24 h.

In the second group, the neural progenitor medium on the NPC-alginate beads was replaced with IHA-IDH1-WT conditioned medium after 24 h. Three to four milliliters of medium was withdrawn from the plates, and four to five milliliters of fresh IHA-IDH1-WT conditioned medium was added every three days for 14 days.

In the third group, the neural progenitor medium on the NPC -alginate beads was replaced with IHA-IDH1-R132H conditioned medium after 24 h. Three to four milliliters of medium was withdrawn from the plates, and four to five milliliters of fresh IHA-IDH1-R132H conditioned medium was added every three days for 14 days.

In the fourth and fifth groups, after 14 days, IHA-IDH1-WT and IHA-IDH1-R132H conditioned mediums on NPC- alginate beads were replaced with neural progenitor medium, and for 3 days, NPCs alginate beads were incubated separately for 3 days at 37 °C and 5% CO₂.

Recovering cells from alginate beads for further experiments

0.5 M ethylenediaminetetraacetic acid (Invitrogen, Cat No: 15575-020) was added to the culture medium containing NPC-alginate beads to disrupt the alginate polymer by Ca²⁺ chelation. After alginate was dissolved, the solution in the plate was transferred to a 50-mL canonical tube. Cells were pelleted by centrifugation at 300 g for 5 min and washed with DMEM-F12 medium. Next, the supernatant was completely removed and discarded. TRI Reagent (Sigma, Cat No: 93289-100ML) was added to the cells to be used for RNA isolation and stored at -80 °C.

RNA isolation and real-time quantitative PCR

Cells recovered from beads on days 0 and 17 were lysed in TRI reagent. The Direct-zol RNA MiniPrep Plus Kit (Zymo Research, Cat No: R2072) was used to isolate RNA. RNA concentration was determined using a Nanodrop (Thermo Scientific, Nanodrop 2000 spectrometer).

cDNA was synthesized from extracted RNA using ProtoScript[®] First Strand cDNA Synthesis Kit (New England BioLabs, Cat No: E6300S). GoTaq[®] qPCR Master Mix (Promega, Cat No: A6001) and Real-Time PCR Detection System (Applied Biosystems 7500 Fast Instrument) were used according to the manufacturers' instructions. The primers are listed in Table 1. GAPDH, a housekeeping gene, was used to normalize changes in specific gene expression.

Results

Generation and characterization of hiPSC-derived hNPCs

To differentiate hiPSCs from NPCs, dual SMAD inhibition of iPSCs in monolayer culture conditions was performed using STEMdiff reagents. Upon the induction of differentiation using the neural induction medium in the presence of SMADi, the neural progenitor medium was used to expand the generated NPCs. Figure 1A illustrates the morphological changes in cells throughout the differentiation process. (Figure 1A). Morphological differences between hiPSCs and hiPSC-derived NPCs were readily visible (Figure 1B).

Table 1. Primer list for RT-qPCR		
Primer name	Forward primer sequence	Reverse primer sequence
TET1	CAGAACCTAAACCACCGTG	TGCTTCGTAGCGCCATTGTAA
MEOX2	GTCAGAAGTCAACAGCAAACCCAG	CACATTCACCAGTTCCTTTTCCCGAGCC
GAPDH	TGCACCACCAACTGCTTAGC	GGCATGGACTGTGGTCATGAG

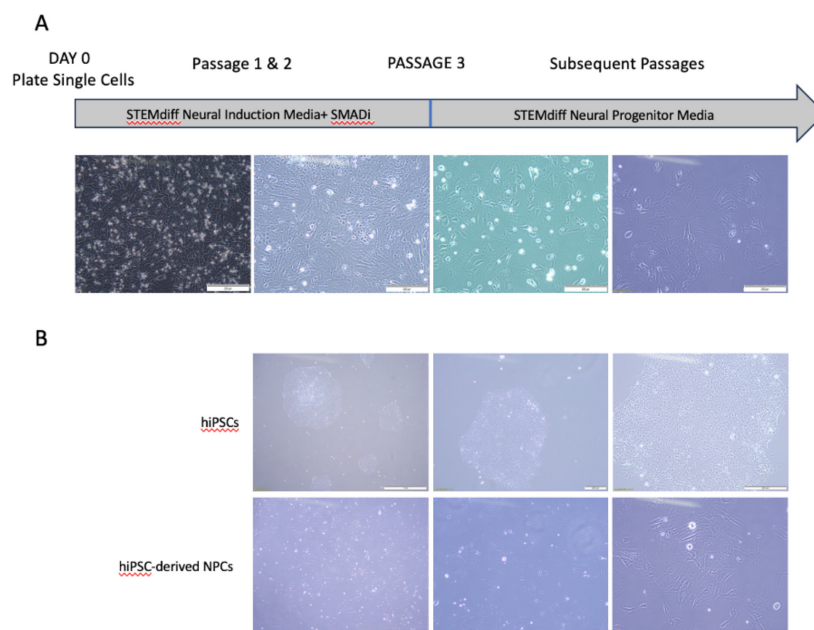


Figure 1. Generation of human NPCs from hiPSCs. A. Images were taken during various stages of hNPC differentiation and show the cell morphology during each differentiation step. Scale bar: 200 μm B. Representative images of hiPSC colonies and iPSC-derived NPCs. Scale bar: 1 mm, 200 μm and 200 μm respectively

Immunocytochemical staining was performed to characterize whether hiPSC-differentiated cells corresponded to NPCs. However, before starting differentiation, we checked whether the hiPSCs to be used for differentiation into NPCs were still pluripotent. OCT4 (encoded by *POU5F1*, also known as Oct3, Oct 3/4), a member of the POU transcription factor family, is an ESC- and germline-specific transcription factor. OCT4 plays a critical role in the maintenance of pluripotency and self-renewal of embryonic stem cells (ESCs)⁽³⁰⁾ and is highly expressed in pluripotent cells, whereas its expression decreases during differentiation⁽³¹⁾. Therefore, hiPSCs were stained with an antibody against the pluripotency marker OCT4, and as expected, all cells were strongly stained for OCT4 (Figure 2A).

Following the confirmation of hiPSC pluripotency, differentiation was initiated, and at the end of the differentiation process, cells were stained for neuroectodermal stem cell markers, namely NESTIN, SRY homology box 1 (SOX1), SRY homology box 2 (SOX2), and paired box 6 protein (PAX6), and the pluripotency marker OCT4 (Figure 2B).

The type IV intermediate filament protein NESTIN is specifically expressed in NPCs and is a well-known neural stem cell marker. It is not expressed in post-mitotic neurons or glia⁽³²⁾. SOX1, a member of the B1 group of the SRY homology box (SOX) transcription factor family, is an important regulator in the fate determination of neural lineage cells and is used to identify NPCs⁽³³⁾. Sex-determining region Y-box2 (SOX2), which is also a member of the SOX family of transcription factors, plays a crucial role in the control of pluripotency, the neural differentiation of pluripotent stem cells, and the self-renewal of neural progenitor stem cells^(34,35). The PAX6 is a transcription factor that plays an important role in the development of the central nervous system, particularly of the eye, spinal cord, and cerebral cortex⁽³⁶⁾. PAX6 regulates many vital aspects of NSCs, such as proliferation, self-renewal, differentiation, and apoptosis.

We found that most of the NPCs stained positively with neuroectodermal stem cell markers. In addition, the cells were not stained with OCT4, as expected. These results indicated that most hiPSCs differentiated into NPCs successfully (Figure 2B).

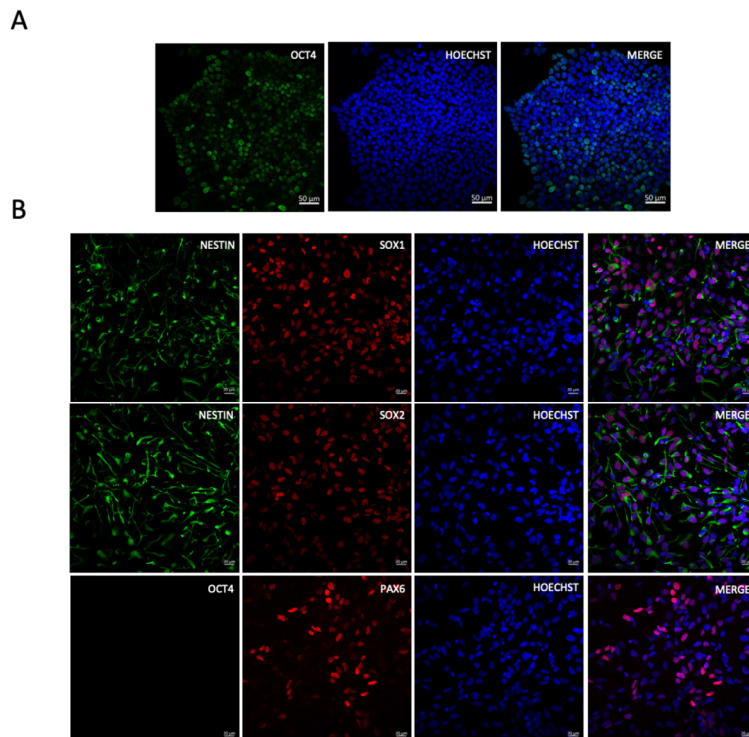


Figure 2. Characterization of hiPSCs and hiPSC-derived NPCs. Representative cells from hiPSCs and hiPSC-derived NPCs were fixed and stained with antibodies against lineage-specific marker proteins. A. hiPSCs express the pluripotency marker OCT4. Scale bar: 50 μ m. B. Immunocytochemical staining showing hiPSC-derived NPCs expressing SOX2, SOX1, PAX6, and nestin. For NPCs, three different co-stainings were performed. 1: Nestin (Green), SOX1 (Red) and Hoechst (Blue). 2: Nestin (Green), SOX2 (Red) and Hoechst (Blue). 3: OCT4 (Green), PAX6 (Red) and Hoechst (Blue). Nuclei were stained with Hoechst 33258. Scale bar: 20 μ m

Alginate bead-based 3D NPC culture

Human NPCs that had been homogeneously dispersed were encapsulated inside alginate hydrogel sphere-like beads. Alginate is widely used in the creation of 3D cell culture models because of its advantageous properties, such as easy gelling under physiological conditions, easy dissolution, ease of microscopic observation, and a structure that allows efficient nutrient and waste diffusion^(37,38).

The concentration of alginate is important for mechanical stability, flexibility, and nutrient diffusion when creating a 3D culture^(38,39). It was observed that alginate beads prepared at low alginate concentrations had large pore sizes, a weak structure, and failed to maintain integrity during long-term culture. It was also reported that the proliferation of ESCs was inhibited in alginate beads prepared at a concentration of 2%, whereas the beads prepared at 1% alginate concentration are the most suitable for ESC growth⁽³⁸⁾.

Therefore, 3D culture was created with 1% alginate to maintain cell viability and proliferation of NPCs. Three different time points and 5 different experimental conditions were selected to develop the model (Figure 3).

Alginate beads formed with NPCs on day 0 were incubated in neural progenitor medium for 24 h (Figure 4A). On day 14, we had two different experimental groups: the first was cultured with a medium collected from IHAs, inducibly expressing IDH1-WT for 14 days. The second was cultured with medium collected from IHAs expressing IDH1-R132H for 14 days. On day 17, we had two experimental groups: i) conditioned medium collected from IHAs inducibly expressing IDH1-WT was removed from NPC-alginate beads on day 14 and neural progenitor medium was added, and cells were cultured with neural progenitor medium for 3 days (until day 17), ii) conditioned medium collected from IHAs inducibly expressing IDH1-R132H was removed from NPC-alginate beads on day 14 and neural progenitor medium was added,

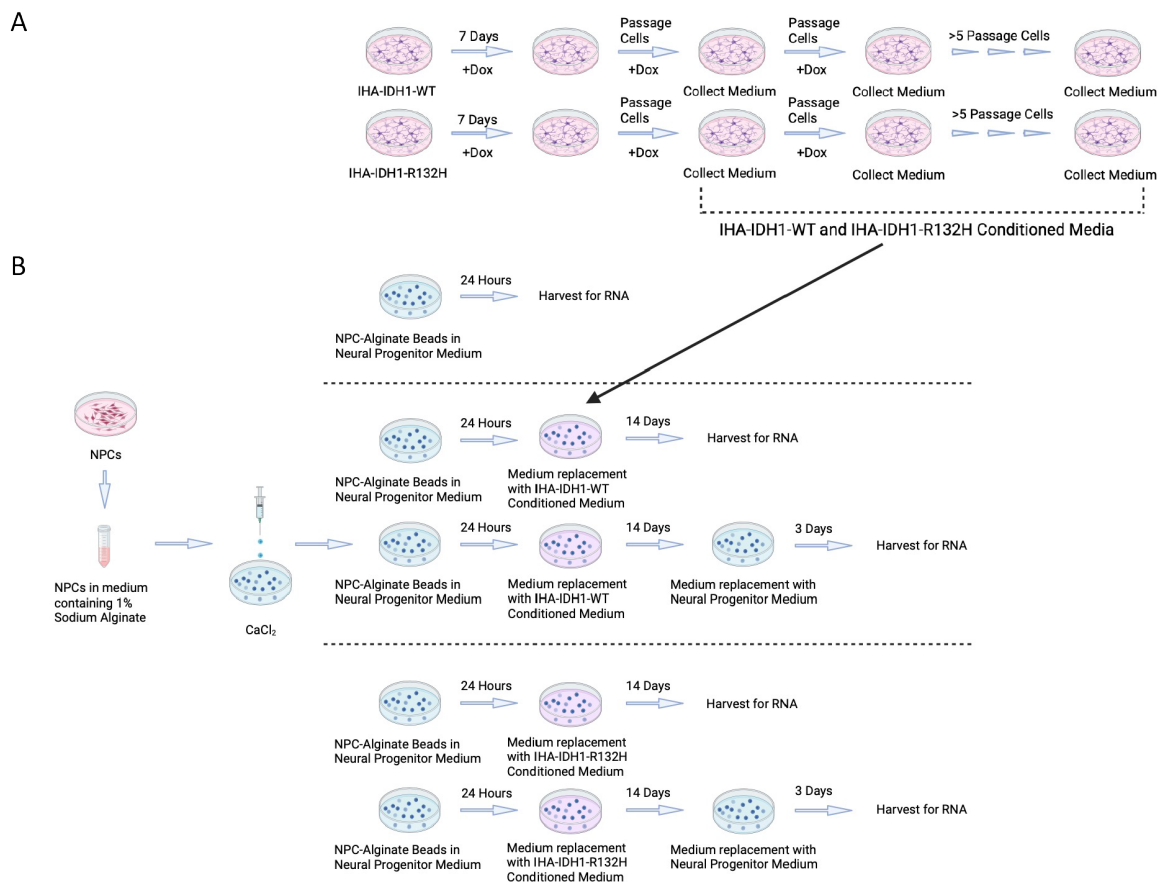


Figure 3. Schematic representation of experimental design A) IHA-IDH1-WT and IHA-IDH1-R132H conditioned media production B) Preparation of 5 experimental conditions: NPC-Control-Day 0, NPC-IDH1_WT-Day 14, NPC-IDH1_R132H-Day 14, NPC-IDH1_WT-Day 17, and NPC-IDH1_R132H-Day 17

and cells were cultured with neural progenitor medium for 3 days (until day 17).

At day 0, the alginate beads were transparent and shiny (Figure 4A). No degradation of the beads was observed on day 0, but on day 14, the beads treated with IHA-IDH1-WT and IHA-IDH1-R132H mediums began to deteriorate. However, the cells within the beads continued to proliferate, forming an aggregate. Deterioration of more beads was observed in day 17 groups; more frequent clustering was observed because of the increase in the number of cells. In addition, it was observed that cells escaped from the beads because of deterioration of the alginate beads in the 14th and 17th day groups (Figure 4B).

To confirm that NPCs exposed to IHA-R132H-conditioned medium display alterations observed in IDH1-R132H-expressing glial cells, we analyzed the expression levels of genes known to be upregulated (*TET1*) and downregulated (*MEOX2*) by IDH1-R132H in NPCs at two time points (day 0 and day 17) by RT-qPCR.

Cells were recovered from the beads at the indicated time points, and the expression of *TET1* and *MEOX2* was examined. On the third day after returning the cells to the neural progenitor medium (day 17), the expression level of *TET1* in NPCs exposed to IHA-IDH1-WT conditioned medium was almost the same as that in day 0 NPCs. On the other hand, it was observed that in the NPCs exposed to IHA-IDH1-R132H conditioned medium, *TET1* expression increased almost

3.5 times compared with that on day 0. Furthermore, a significant difference in *TET1* expression was observed when NPC-IDH1_R132H-Day17 cells were compared with NPC-IDH1_WT-Day17 cells (Figure 5A). Therefore, we conclude that growing NPCs in IHA-IDH1-R132H conditioned medium induces the expression of *TET1*, in line with the reported induction of *TET1* in IDH1/2 mutant gliomas⁽⁴⁰⁾.

On the other hand, it was observed that *MEOX2* expression was suppressed both in NPCs cultured in IHA-IDH1-R132H conditioned medium and in IHA-IDH1-WT conditioned medium. However, suppression tended to be stronger in NPCs cultured in IHA-IDH1-R132H conditioned medium compared with the IHA-IDH1-WT conditioned medium (2.2 fold, $p=0.21$, after multiple-test correction in ANOVA) (Figure 5B).

Discussion

Mutant IDH1/2 expression or exposure to D-2-HG leads to the G-CIMP phenotype in different cell types and drives the cells to a less differentiated point⁽¹⁴⁾. However, most in vitro studies of gliomas rely on tumor cells cultured in 2D environments and may not fully recapitulate the 3D tumor microenvironment. Therefore, the characterization of early epigenomic changes resulting from IDH1/2 mutations in non-tumor cells, including analysis of major histone modifications, DNA methylation, and transcriptome, has largely been performed in cells cultured in 2D. In addition,

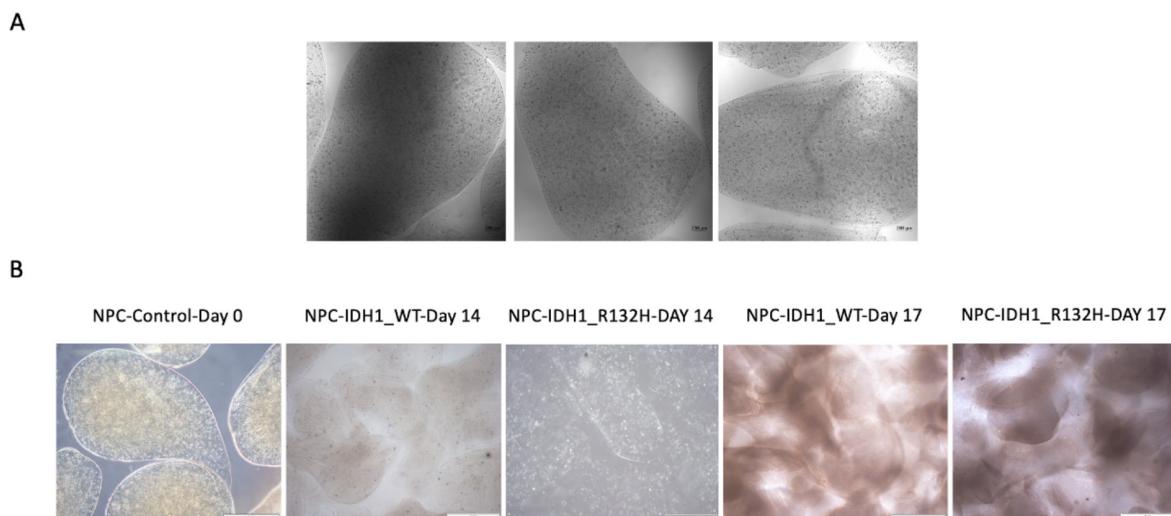


Figure 4. 3D culture of hNPCs in alginate beads. A. Confocal microscopy images of alginate-based 3D NPC culture on day 1. Scale bars: 500 μ m. B. Light microscope images of alginate-based 3D NPC cultures at day 0 (in NPC medium), day 14 (in IHA-IDH1-WT and IHA-IDH1-R132H conditioned-medium), and day 17. On day 14, IHA-IDH1-WT and IHA-IDH1-R132H conditioned medium were changed with regular NPC medium and cultured for three days before imaging on day 17. Scale bar: 1 mm

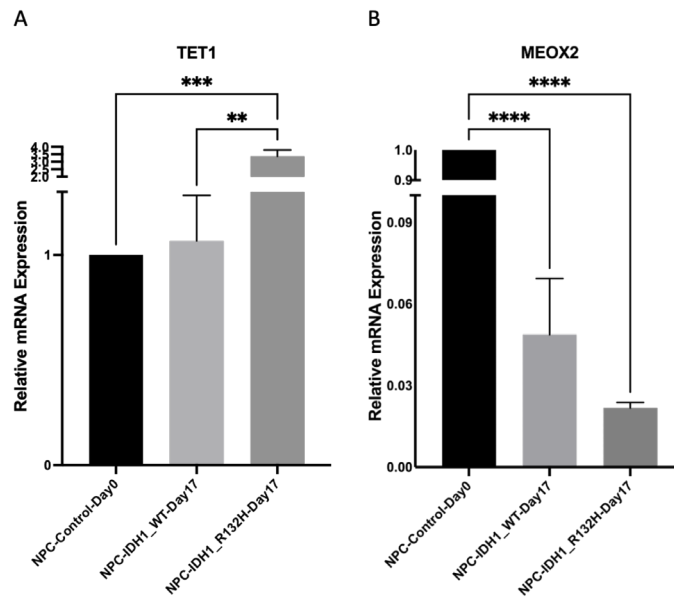


Figure 5. Expression patterns of TET1 and *MEOX2* genes. (A) TET1 and (B) *MEOX2* mRNA levels were analyzed by RT-qPCR in NPCs cultured inside alginate beads under three different experimental conditions. *GAPDH* was used as the housekeeping gene. **p <0.01; ***p <0.001; ****p <0.0001.

some of these studies were conducted under cell culture conditions with heterogeneous tumor samples or cells (e.g., astrocyte) that could not fully reflect the glioma biology occurring in three-dimensional tissue. However, IDH1/2 mutations are genetic changes that occur at the earliest stages of gliomagenesis, when other oncogenic changes are not yet present.

Another factor to be considered when creating glioma models is the "cell-of-origin" problem. NSCs, which have self-renewal properties, are considered ideal candidates as the origin cells of gliomas because of their development potential and plasticity properties. NPCs are also produced by NSCs to produce progeny along neuronal and glial lineages⁽²⁰⁾. Although gliomas result from the accumulation of mutations in neural stem/progenitor cells, oligodendrocyte progenitor cells, or the dedifferentiation of astrocytes, most cell culture models of gliomas rely on tumor cell lines generated from high-grade tumor tissues⁽²⁰⁾. Because these cells are more likely to reflect the cellular states in full-blown tumors, rather than the earliest cells of origin that give rise to gliomas, they are not suitable for modeling the early stages of gliomas. As the likely cells-of-origin, NPCs could better reflect the cellular states at the initial stages of gliogenesis, and some features associated with gliogenesis can be better understood in these cells, which could lead to the development of more effective therapies. It is critical

that the model in which the analysis will be performed is capable of reflecting the earliest stages of glioma, in which IDH mutations exert their effects, and that it can be easily intervened under controlled conditions. Therefore, human induced pluripotent stem cell (hiPSC)-derived NPCs with no oncogenic mutation were used. The ability of iPSCs produced from non-pluripotent cells to differentiate into different cell types, including neurons, has enabled the development of better disease models that could be used for studying disease etiopathogenesis and developing novel therapies, either using cells from healthy donors or patient-derived cells^(41,42).

To develop a model based on hiPSC-derived NPCs, we needed a source for IDH1 mutations. One way to achieve this could be the introduction of the mutant IDH1 into NPCs and engineering them to express it either in a constitutive or inducible manner. However, the former would not allow us to investigate the immediate effects of IDH1, whereas the latter may suffer from leaky expression leading to possibly irreversible epigenomic changes. Therefore, we sought to expose NPCs to conditions that could mimic IDH1-R132H-induced alterations. To this end, we used IHAs that inducibly expressed IDH1-R132H, and as a control, we used IHAs that inducibly expressed WT IDH1. Because the immortalized human astrocyte cells used to produce the IHA-IDH1-WT and IHA-IDH1-R132H condition mediums were generated by

infection with pLVX-Tet-On retroviruses, they can be induced with doxycycline to produce IDH1-WT or IDH1-R132H⁽⁴³⁾. In addition to expressing E6/E7, these cells were also infected with hTERT⁽⁴⁴⁾. Although these cells were previously used to characterize early epigenomic changes in gliomas, their expression of E6/E7 and particularly hTERT, one of the defining early mutations of oligodendrogliomas and GBMs, may not reflect the earliest cell state that precedes IDH1/2 mutations. However, they could still be used as a source of 2-HG and other IDH mutation-induced cellular alterations that are released into the culture medium. Therefore, we used these IHAs that express IDH1-R132H to generate the conditioned medium and IHAs that express WT-IDH1 to generate the control conditioned medium in our model.

Many of the most recently cited protocols for the production of NPCs are monolayer and embryoid body protocols. In both protocols, NPC generation from iPSCs takes 21-30 days⁽⁴⁵⁾. In this study, the monolayer protocol was implemented to generate NPCs from healthy iPSCs. NPC markers such as NESTIN, PAX6, SOX1, SOX2, and DACH1 should be expressed in iPSC-derived NPCs, whereas pluripotency markers such as OCT4, NANOG, DNMT3B, and DPPA4 should be downregulated. In addition, these cells continue to maintain their morphology and multipotential identity after freezing and thawing⁽⁴⁶⁾. Characterization of NPCs and iPSCs used in this study was demonstrated by immunohistochemical staining. Cells differentiated into iPSCs with the STEMdiff™ monolayer culture protocol lost the pluripotency marker OCT4 and were positive for NESTIN, PAX6, SOX1, and SOX2.

2D culture systems cannot fully provide the physiological environment faced by tumor cells *in vivo*. To better reflect the cell-cell and cell-ECM interactions, biomaterials are good candidates for mimicking *in vivo* conditions *in vitro*. Alginate is a polymer that is readily available, economical, has long-term stability and water retention, and has the advantages of biocompatibility, biodegradability, and nontoxicity^(47,48). Because alginate-based hydrogels have several such preferable properties, they are widely used as scaffolds in processes such as cell encapsulation and tissue engineering⁽⁴⁹⁾.

A 3D glioblastoma cell culture model was developed with U87 glioblastoma cells and alginate microfibers, which mimics the treatment conditions used in drug response studies⁽⁵⁰⁾. Cells in 3D alginate culture treated with temozolomide showed an anti-proliferative effect similar to that in 2D cell

culture medium. On the other hand, when compared with 2D cell culture, it was determined that the expression of genes related to drug resistance increased more in 3D alginate culture. The alginate-based 3D culture model has been proposed as a fast, reliable, and practical model for drug testing and therapy development⁽⁵⁰⁾.

In our study to make alginate-based 3D culture, the bead generation protocol was used⁽⁵¹⁾. The alginate beads were approximately 2 mm in diameter, and each bead contained approximately 2500 cells. For the first time in the literature, we show that alginate allows the survival and growth of encapsulated NPCs during the culture period (18 days). From the first day of culture, the cells increased in number and formed dense clusters. We observed that the alginate beads swelled and did not deteriorate as the number of cells increased.

One of the two genes we selected to confirm their altered expression in response to IDH1-R132H-expressing IHA conditioned medium was Tet methylcytosine dioxygenase 1 (*TET1*). D-2-HG, an α -KG antagonist, competitively inhibits α -KG-dependent dioxygenases, including the Ten-Eleven Translocation (TET) family. *TET1* is a member of the TET family that catalyzes the conversion of 5-methylcytosine (5mC) to 5-hydroxymethylcytosine⁽⁵²⁾. *TET1* deficiency is associated with greater genomic instability in glioma cell lines and increases resistance to ionizing radiation therapy. Furthermore, the amount of *TET1* expression varies according to the histological type of the disease. Importantly, it is expressed at higher levels in IDH-mutant low-grade gliomas and IDH-mutant GBMs than in IDH (WT) LGGs and GBMs⁽⁴⁰⁾, which makes it an ideal gene to test in our model.

Mesenchyme Homeobox 2 (*MEOX2* or *GAX*), a member of the Homeobox gene family, activates p16 and p21; therefore, overexpression of *MEOX2* stops growth and causes endothelial cell senescence⁽⁵³⁾. *MEOX2* expression is permanently suppressed in immortalized human astrocyte cells that express IDH1-R132H⁽⁴³⁾. Therefore, we selected *MEOX2* as another gene to test our model. RT-qPCR analysis of *TET1* and *MEOX2* at two time points (day 0 and day 17) in NPCs exposed to IHA-IDH1-R132H or IHA-IDH1-WT conditioned medium yielded results that are consistent with the literature, albeit *MEOX2* expression change not reaching statistical significance ($p=0.21$), possibly due to low replicate number ($n=2$).

Conclusion

On the basis of our findings in this study, we conclude that the alginate-based 3D NPC culture model exposed to IHA-conditioned media is suitable for studying the effects of IDH mutations on the earliest stages of gliomas, without the confounding effects of other oncogenic mutations. Further characterization of NPCs could reveal the effects of 3D culture compared with 2D culture and establish this novel model for further epigenomic investigations of gliomas.

Ethics

Ethics Committee Approval: Ethical approval for the study was obtained from İzmir Biomedicine and Genome Center Non-Invasive Research Ethics Committee (ethical approval number: 2020-042).

Informed Consent: iPSCs were purchased from Applied Stem Cell (Cat No: ASE-9202)

Peer-review: Externally peer-reviewed.

Authorship Contributions

Concept: B.E., T.Y., Y.O., Design: B.E., Y.O., Data Collection or Processing: B.E., T.Y., Analysis or Interpretation: B.E., T.Y., Y.O., Literature Search: B.E., Y.O., Writing: B.E., T.Y., Y.O.

Conflict of Interest: No conflict of interest was declared by the authors.

Financial Disclosure: This study was supported by TÜBİTAK grant #1172981 and #2145097.

References

- González-Castro TB, Juárez-Rojop IE, López-Narváez ML, et al. Genetic Polymorphisms of CCDC26 rs891835, rs6470745, and rs55705857 in Glioma Risk: A Systematic Review and Meta-analysis. *Biochem Genet* 2019;57:583-605.
- Sung H, Ferlay J, Siegel RL, et al. Global Cancer Statistics 2020: GLOBOCAN Estimates of Incidence and Mortality Worldwide for 36 Cancers in 185 Countries. *CA Cancer J Clin* 2021;71:209-49.
- Haddock S, Alban TJ, Turcan Ş, et al. Phenotypic and molecular states of IDH1 mutation-induced CD24-positive glioma stem-like cells. *Neoplasia (United States)* 2022;28:100790.
- Xu S, Tang L, Li X, Fan F, Liu Z. Immunotherapy for glioma: Current management and future application. *Cancer Lett* 2020;476:1-12.
- Stupp R, Mason WP, Van Den Bent MJ, et al. Radiotherapy plus Concomitant and Adjuvant Temozolomide for Glioblastoma. *N Engl J Med* 2005;352:987-96.
- Yang K, Wu Z, Zhang H, et al. Glioma targeted therapy: insight into future of molecular approaches. *Mol Cancer* 2002;21:39.
- Bush NAO, Chang SM, Berger MS. Current and future strategies for treatment of glioma. *Neurosurg Rev* 2017;40:1-14.
- Dang L, White DW, Gross S, et al. Cancer-associated IDH1 mutations produce 2-hydroxyglutarate. *Nature* 2009;462:739-44.
- Louis DN, Perry A, Wesseling P, et al. The 2021 WHO classification of tumors of the central nervous system: a summary. *Neuro Oncol* 2021;23:1231-51.
- Yan H, Williams D, Jin G, et al. IDH1 and IDH2 mutations in gliomas. *N Engl J Med* 2009;360:765-73.
- Chowdhury R, Yeoh KK, Tian YM, et al. The oncometabolite 2-hydroxyglutarate inhibits histone lysine demethylases. *EMBO Rep* 2011;12:463-9.
- Xu W, Yang H, Liu Y, et al. Oncometabolite 2-hydroxyglutarate is a competitive inhibitor of α -ketoglutarate-dependent dioxygenases. *Cancer Cell* 2011;19:17-30.
- Lu C, Ward PS, Kapoor GS, et al. IDH mutation impairs histone demethylation and results in a block to cell differentiation. *Nature* 2012;483:474-8.
- Turcan S, Rohle D, Goenka A, et al. IDH1 mutation is sufficient to establish the glioma hypermethylator phenotype. *Nature* 2012;483:479-83.
- Oktay Y, Ülgen E, Can Ö, et al. IDH-mutant glioma specific association of rs55705857 located at 8q24.21 involves MYC deregulation. *Sci Rep* 2016;6:27569.
- Suzuki H, Aoki K, Chiba K, et al. Mutational landscape and clonal architecture in grade II and III gliomas. *Nat Genet* 2015;47:458-68.
- Jiang Y, Uhrbom L. On the origin of glioma. *Ups J Med Sci* 2012;117:113-21.
- Doetsch F, Caillé I, Lim DA, Manuel García-Verdugo J, Alvarez-Buylla A. Subventricular Zone Astrocytes Are Neural Stem Cells in the Adult Mammalian Brain. *Cell*. 1999;97:703-16.
- Mich JK, Signer RAJ, Nakada D, et al. Prospective identification of functionally distinct stem cells and neurosphere-initiating cells in adult mouse forebrain. *Elife* 2014;3:e02669.
- Cahill D, Turcan S. Origin of Gliomas. *Semin Neurol* 2018;38:5-10.
- Lee JH, Lee JH. The origin-of-cell harboring cancer-driving mutations in human glioblastoma. *BMB Rep* 2018;51:481-3.
- Engineering 3D Tissue Systems to Better Mimic Human Biology [Internet]. Available from: <https://www.researchgate.net/publication/245161944>
- Lee J, Cuddihy MJ, Kotov NA. Three-dimensional cell culture matrices: state of the art. *Tissue Eng Part B Rev* 2008;14:61-86.
- Albrecht DR, Underhill GH, Wassermann TB, Sah RL, Bhatia SN. Probing the role of multicellular organization in three-dimensional microenvironments. *Nat Methods* 2006;3:369-75.
- Beningo KA, Dembo M, Wang YL. Responses of fibroblasts to anchorage of dorsal extracellular matrix receptors. *PNAS* 2004;101:18024-9.
- Discher DE, Janmey P, Wang YL. Tissue Cells Feel and Respond to the Stiffness of. *Science* 2005;310:1139-43.
- Choukaife H, Doolaanea AA, Alfatama M. Alginate nanoformulation: Influence of process and selected variables. *Pharmaceuticals (Basel)* 2020;13:335.
- Bozza A, Coates EE, Incitti T, et al. Neural differentiation of pluripotent cells in 3D alginate-based cultures. *Biomaterials* 2014;35:4636-45.
- Li L, Davidovich AE, Schloss JM, et al. Neural lineage differentiation of embryonic stem cells within alginate microbeads. *Biomaterials* 2011;32:4489-97.
- Mehravar M, Ghaemimanesh F, Poursani EM. An Overview on the Complexity of OCT4: at the Level of DNA, RNA and Protein. *Stem Cell Rev Rep* 2021;17:1121-36.
- Schoorlemmer J, Jonk L, Shen S, Van Puijenbroek A, Feijen A, Kruijer W. Regulation of Oct-4 gene expression during differentiation of EC cells. Vol. 21, *Molecular Biology Reports*. Mol Biol Rep 1995;21:129-40.

32. Lendahl U, Zimmerman LB, McKay RDG. CNS Stem Cells Express a New Class of Intermediate Filament Protein. *Cell* 1990;60:585-95.
33. Venere M, Han YG, Bell R, Song JS, Alvarez-Buylla A, Bletloch R. Sox1 marks an activated neural stem/progenitor cell in the hippocampus. *Development* 2012;139:3938-49.
34. Ring KL, Tong LM, Balestra ME, et al. Direct reprogramming of mouse and human fibroblasts into multipotent neural stem cells with a single factor. *Cell Stem Cell* 2012;11:100-9.
35. Zhang S. Sox2, a key factor in the regulation of pluripotency and neural differentiation. *World J Stem Cells* 2014;6:305-11.
36. Simpson TI, Price DJ. Pax6; a pleiotropic player in development. *Bioessays* 2002;24:1041-51.
37. Andersen T, Auk-Emblem P, Dornish M. 3D Cell Culture in Alginate Hydrogels. *Microarrays (Basel)* 2015;4:133-61.
38. Wang N, Adams G, BATTERY L, Falcone FH, Stolnik S. Alginate encapsulation technology supports embryonic stem cells differentiation into insulin-producing cells. *J Biotechnol* 2009;144:304-12.
39. Saha K, Keung AJ, Irwin EF, et al. Substrate modulus directs neural stem cell behavior. *Biophys J* 2008;95:4426-38.
40. Luechtefeld T, Lin N, Paller C, Kuhns K, Laterra JJ, Bressler JP. Measuring Cancer Hallmark Mediation of the TET1 Glioma Survival Effect with Linked Neural-Network Based Mediation Experiments. *Sci Rep* 2020;10:8886.
41. Csete M. Translational prospects for human induced pluripotent stem cells. *Regen Med* 2010;5:509-19.
42. Raya A, Rodríguez-Pizà I, Guenechea G, et al. Disease-corrected haematopoietic progenitors from Fanconi anaemia induced pluripotent stem cells. *Nature* 2009;460:53-9.
43. Turcan S, Makarov V, Taranda J, et al. Mutant-IDH1-dependent chromatin state reprogramming, reversibility, and persistence. *Nat Genet* 2018;50:62-72.
44. Sonoda Y, Ozawa T, Hirose Y, et al. Formation of Intracranial Tumors by Genetically Modified Human Astrocytes Defines Four Pathways Critical in the Development of Human Anaplastic Astrocytoma. *Cancer Res* 2001;61:4956-60.
45. Bell S, Hettige NC, Silveira H, et al. Differentiation of Human Induced Pluripotent Stem Cells (iPSCs) into an Effective Model of Forebrain Neural Progenitor Cells and Mature Neurons. *Bio Protoc* 2019;9:e3188.
46. Zink A, Lisowski P, Prigione A. Generation of Human iPSC-derived Neural Progenitor Cells (NPCs) as Drug Discovery Model for Neurological and Mitochondrial Disorders. *Bio Protoc* 2021;11:e3939.
47. Łabowska MB, Cierluk K, Jankowska AM, Kulbacka J, Detyna J, Michalak I. A review on the adaptation of alginate-gelatin hydrogels for 3D cultures and bioprinting. *(Basel)* 202;14:858.
48. Reig-Vano B, Tylkowski B, Montané X, Giamberini M. Alginate-based hydrogels for cancer therapy and research. *Int J Biol Macromol* 2021;170:424-36.
49. Liu Y, Song B, Chen X, Cai Q, Tian W. Alginate-based hydrogels encapsulated TWS119 for inducing neuronal differentiation of neural stem cells. *J Biomater Tissue Eng* 2014;4:1087-92.
50. Dragoj M, Stojkowska J, Stanković T, et al. Development and validation of a long-term 3d glioblastoma cell culture in alginate microfibers as a novel bio-mimicking model system for preclinical drug testing. *Brain Sci* 2021;11:1025.
51. Davoudi F, Ghorbanpoor S, Yoda S, et al. Alginate-based 3D cancer cell culture for therapeutic response modeling. *STAR Protoc* 2021;2:100391.
52. Wu X, Zhang Y. TET-mediated active DNA demethylation: Mechanism, function and beyond. *Nat Rev Genet* 2017;18:517-34.
53. Douville JM, Cheung DYC, Herbert KL, Moffatt T, Wigle JT. Mechanisms of MEOX1 and MEOX2 regulation of the cyclin dependent kinase inhibitors p21 CIP1/WAF1 and p16 INK4a in vascular endothelial cells. *PLoS One* 2011;6:e29099.